Chapter 29

Excitation Energy Transfer Between (Bacterio)Chlorophylls—the Role of Excitonic Coupling

Dieter Leupold*
Institut für Physik/Photonik, Universität Potsdam, Postfach 601553, D-14415 Potsdam, Germany

Heiko Lokstein*
Institut für Biochemie und Biologie/Pflanzenphysiologie, Universität Potsdam, Karl-Liebknecht-Str. 24-25, D-14476 Golm, Germany

Hugo Scheer
Department Biologie I – Botanik, Universität München, Menzinger Strasse 67, D-80683 München, Germany

Summary

The function of photosynthetic light harvesting complexes (LHCs) comprises absorption and regulated excitation energy transfer (EET) to the photochemical reaction centers (RCs). Photosynthesizing organisms have developed a variety of LHCs but, apart from phycobilins in cyanobacteria and certain algae, use only two types of pigments, (bacterio)chlorophylls ((B)Chl) and carotenoids. Adaptation of their electronic excited state properties to the requirements of efficient, yet safe light harvesting is realized by pigment-protein as well as pigment-pigment interactions, thereby varying: i) the mutual orientations and distances of the pigments; and,

*Authors for correspondence, email: dieter.e.leupold@web.de, lokstein@rz.uni-potsdam.de

Bernhard Grimm, Robert J. Porra, Wolfhart Rüdiger and Hugo Scheer (eds): Chlorophylls and Bacteriochlorophylls: Biochemistry, Biophysics, Functions and Applications, pp. 413–430.

ii) the pigments' local environments. This will be exemplified for the seemingly irregular (B)Chl networks of the main light-harvesting complex (LHC II) of higher plants and the so-called Fenna-Matthews-Olsen-Protein (FMO) of green photosynthetic bacteria, and the highly-ordered BChl arrangements in the LH2 antenna of purple bacteria and in chlorosomes of green bacteria. The occurrence and extent of excitons will be discussed.

I. Introduction

The two essential functions of (bacterio)chlorophylls ((B)Chls) in photosynthetic light harvesting complexes (LHCs) are absorption of light and subsequent electronic excitation energy transfer (EET) to a photosynthetic reaction center (RC). The latter can also absorb light, but such events occur at rates <10 Hz whereas the RC can turn over excitations at rates around 1000 Hz (Mauzerall and Greenbaum, 1989). LHCs deliver excitation energy to the RCs to assure optimal performance according to the external and internal conditions. Isolated (B)Chls, however, do not harvest light efficiently: they absorb light only in narrow regions of the spectrum, the electronic excitation energy is partly lost as heat (especially in aggregates), and potentially dangerous triplet states are formed by intersystem crossing (ISC). LHCs have evolved to minimize and control these losses in efficient EET arrays. While using relatively small amounts of protein, they broaden or extend the (B)Chl absorption regions and reduce wasteful and dangerous ISC to (B)Chl triplets, thereby increasing safely the effective cross section for absorption of the RC by orders of magnitude.

Remarkable progress has been achieved in understanding photosynthetic EET processes. In particular, LH2 of purple bacteria of which detailed structural, spectroscopic and biochemical information is available, has triggered various theoretical investigations which, in turn, inspired further experiments. A nearly complete picture of EET through the bacterial photosynthetic unit (PSU) has been proposed (Hu et al., 2002). Such a model is still lacking for the main light-harvesting complex II (LHC II) of higher plants and, also for EET through Photosystem (PS) II and PS I.

In LHC, there are two extreme cases of EET between donor (D) and acceptor (A), depending on their transition-dipole coupling: there can be 'hopping' of a completely localized excitation (weak coupling, Förster transfer), or coherent exciton motion with delocalization of excitation (strong coupling). In the case of intermediate coupling, EET may start with coherent motion, which is quickly perturbed by vibrations (called partial exciton) or coherence may be lost early, so that EET and vibrational relaxation coincide (hot transfer; Kimura et al., 2000).

In LHCs all these modes of EET have been observed. The known LHC structures show two types of pigment arrangements: highly ordered arrays in purple bacterial LHC (Karrasch et al., 1995; McDermott et al., 1995; Koepke et al., 1996; Robert et al., 2003), or in chlorosomes of green bacteria (Chapter 20, de Boer and de Groot,), as well as arrangements of much lower symmetry in LHCs of higher plants or the Fenna-Matthews-Olsen-protein (FMO) (see Chapter 28, Melkozernov and Blankenship; and Fig. 1 and Color Plate 3 from Chapter 24, Noy et al.) .

In the monomeric subunits of LHC II, 12–15 Chls are located in distinct protein environments. Here, broadening of the absorption regions, compared to monomeric Chl in solution, is assumed to occur mainly as result of heterogeneities caused by site-specific Chl-protein interaction. A similar assumption is made for the FMO complex of green sulfur bacteria.

By contrast, the 24–27 BChl *a* of LH2 are arranged in two distinct, ring-like structures of high symmetry. In one of the compartments, B850, it is not the diversity of BChl-protein interactions which extends the absorption regions, but band broadening and splitting caused by strong pigment-pigment excitonic interactions. Strong pigment-pigment interactions also cause the broad near infrared (NIR) absorptions of chlorosomes, which are nearly devoid of protein

Abbreviations: A – acceptor in EET; BChl – bacteriochlorophyll; BChl-Bxxx – BChl in a complex absorbing at xxx nm; BPhe – bacteriopheophytin; CD – circular dichroism; Chl – chlorophyll; *Chl. – Chlorobium;* CIEM – configuration interaction exciton method; CP29 – minor Photosystem II antenna complex (Lhcb4); D – donor in EET; EET – excitation energy transfer; FMO – Fenna-Matthew-Olsen complex; ISC – intersystem crossing; LH1, LH2 – core and peripheral light-harvesting complexes of purple bacteria, respectively; LHC – light-harvesting complex; LHC II – main light-harvesting complex of higher plants and algae, alternatively also termed LHCB; NIR – near infrared; NLPF – non-linear polarization in the frequency domain; PCP – peridinin chlorophyll *a*-protein; PS – Photosystem; PSU – photosynthetic unit; *Ptc. – Prostecochloris*; *Rba. – Rhodobacter*; *Rps. – Rhodopseudomonas*; *Rsp. – Rhodospirillum*

(Blankenship et al., 1995; Chapter 15, Frigaard et al.; Chapter 20, de Boer and de Groot).

The aforementioned strategies, alone or in combination, are useful not only to broaden the absorption regions, but they may also speed up EET within and between sub-complexes of the respective PS. Light absorption by any of these components with populations of an excited state is generally followed by deactivation to the vibrationally relaxed lowest excited state(s). Then, EET to a spatially and spectrally suitable acceptor (A) in the EET chain takes place with high quantum yield. Hence, EET overcomes the competing deactivation routes by radiative and radiationless processes in the lowest excited singlet state of D. The EET rate, k_{DA}, in case of weak D-A interaction is described:

$$k_{DA} = \frac{2\pi}{\eta}\left|V_{DA}\right|^2 J_{DA} \quad (1)$$

where V_{DA} is the electronic coupling factor. All nuclear factors are contained in the Förster spectral overlap integral J_{DA}. If the distance between D and A is much larger than the size of D and A themselves (long-range transfer), the Coulomb coupling can be expanded into a multipole series and restricted to the dipole-dipole term, which gives the Förster formula:

$$k_{DA} = \frac{9000(\ln 10)\kappa^2\phi_D}{128\pi^5 n^4 N r^6 \tau_D}\int_o^\infty \frac{f_D(\tilde{\nu})\varepsilon_{DA}(\tilde{\nu})}{\tilde{\nu}^4}\, d\tilde{\nu} \quad (2)$$

where κ^2 and r describe the orientation and distance, respectively, of the D and A transition dipoles; ϕ_D and τ_D are fluorescence quantum yield and excited state lifetime, respectively, of D in the absence of A, N is the Avogadro number; $f_D(\tilde{\nu})$ is the normalized fluorescence intensity of D; $\varepsilon_A(\tilde{\nu})$ the extinction coefficient of A at wavenumber $\tilde{\nu}$; and n is the refractive index of the medium in the optical range of the local environment of the D-A pair. Since k_{DA} depends inversely on n^4, determination of n of the respective pigments local environment is of considerable importance for assessment of absolute rates. A broad variety of values and their meaning is found in the literature (Knox and van Amerongen, 2002). Below, we refer to a recently-determined value for n for the local environment responsible for EET 800 → 850 nm in LH2 (n = 1.59; I. Eichwurzel, unpublished), which is similar to that for Chl *a* in the peridinin chlorophyll *a*-protein (PCP) (n = 1.6; Kleima et al., 1997). The weak coupling limit is applicable, at least in good approximation, for most EET processes *between* LHC. It is also applicable for EET to the RC, where relatively long distances prevail in order to prevent electron transfer to the antenna.

II. Excitation Energy Transfer in Purple Bacteria

A. General

A prototypical purple bacterial PS consists of several peripheral light-harvesting complexes, LH2, comprised of 8–9 identical units, each carrying 3 BChl *a* and 1–2 carotenoids. They surround a core antenna (LH1) complex with approximately 16 identical units each carrying 2 BChl *a* and 1 (or more) carotenoid which, in turn, encases the RC (data for the *Rhodopseudomonas* (*Rps.*) *acidophila*-type of purple bacteria; Papiz et al., 1996). Whereas the ratio of RC/LH1 complexes is fixed, the amount of LH2, if present, depends on growth conditions (Georgakopoulou et al., 2002). An important modification of this model is a clustering of LH1-RC complexes in a 'lake' of LH2 (Nagarajan and Parson, 1997). An interrupted ring is found in crystals of LH1-RC-complexes of *Rhodoseudomonas* (*Rps.*) *palustris* (Roszak et al., 2003), and two LH1 complexes, forming an elongated S-shaped super-complex with two RCs, have been seen in bacteria containing the PufX protein (Jungas et al., 1999; Westerhuis et al., 2002; for more details and examples see Hu et al., 2002).

The NIR absorptions differ for LH1 (875 nm) and LH2 (800 and 850 nm) complexes. NIR photons can start the EET chain in either LH1 or LH2, and within the latter at either BChl-B850 or a BChl-B800, resulting in different numbers and types of EET steps before reaching the RC.

B. Light Harvesting Complex 2: Strong and Weak Coupling, Excitation Energy Transfer from Higher Excited States, Deactivation

In LH2, a photon is absorbed by one of the circular aggregates, either BChl-B800 or BChl-B850, or by a carotenoid. It is assumed that Q_y of BChl-B850 is the terminal state for all light-harvesting processes in LH2 and, hence, the donor in EET to LH1.

The following discussion will focus on the Q_y absorptions in the red to NIR region. Investigations

involving higher excited states are scarce, they include EET from higher excited (Soret-region) BChl to carotenoids (Limantara et al., 1998), radiative transitions (low-yield) from B_x and Q_x states of BChl to the ground state (Leupold et al., 2002; D. Leupold et al., unpublished) and processes from higher excited states, which bypass the Q_y excitonic manifold (Limantara et al., 1998). Energy transfer from carotenoids is discussed in Chapter 30 (Koyama and Kakitani).

1. The Q_y-Band Region

Experiments and theoretical description of EET following excitation in the 800 nm-centered absorption band of LH2 (belonging mainly to the monomeric BChl-B800, but see Leupold et al., 1999b) and detection in the 850 nm band have concentrated on LH2 from *Rps. acidophila*, *Rhodobacter* (*Rba.*) *sphaeroides*, and *Rhodospirillum* (*Rsp.*) *molischianum*. LH2s have been classified as either '*acidophila*-like' or '*molischianum*-like', with the main difference in the orientation of the BChl-B800 molecules. LH2 of *Rba. sphaeroides* is disputably grouped to '*molischianum*-like' (Georgakopoulou et al., 2002).

The experimentally determined k_{DA}^{-1} values for EET from BChl-B800 → BChl-B850 at room temperature are 600–900 fs (Table 1). It has been a general problem of Förster-formalism based simulations that, neglecting among other issues (see below) the excitonic level structure, the calculated EET rates were too low by a factor of about 5 (Pullerits et al., 1997). This has been corroborated by a study of B800 → B850 EET with complexes in which BChl-B800 was completely exchanged (Herek et al., 2000), thereby blue-shifting the NIR absorption maximum (originally located at 800 nm) stepswise down to 670 nm, while maintaining the BChl-B850 (see Table 1). The simulated data nicely parallel the experimental increase of transfer times, but are systematically lower by a factor of 5 (Herek et al., 2000). For LH2, precise structural data are available, as well as a wealth of data from linear as well as nonlinear optical spectroscopy. Improved calculations, using the configuration interaction exciton method (CIEM), on LH2 from *Rsp. molischianum* and *Rps. acidophila* by the group of Korppi-Tommola (Linnanto et al., 1999; Linnanto and Korppi-Tomola, 2000; Ihalainen et al., 2001) satisfactorily described many of the experimental data. Important contributions to the recent improvement of the theoretical understanding of light harvesting in LH2 were also provided by Krueger et al. (1998), Cory et al. (1998), Scholes and Fleming (2000), Hu et al. (1997, 2002), Damjanovic et al. (2002), and data derived from single-moleucle spectroscopy (Chapter 21, Köhler and Aartsma). Remaining discrepancies regarding a few experimental results are stimulating for both, theory and experiment.

a. Excitonic Model for B800-B850

Excitonic models for the Q_y transition range of LH2 of *Rps. acidophila* and *Rsp. molischianum* (Cory et al., 1998; Krueger et al. 1998, Linnanato et al., 1999;

Table 1. Experimentally observed and calculated EET time constants for BChl-B800 → BChl-B850 in LH2 of purple bacteria

Antenna complex (modification)	λ_{pump} [nm]	λ_{probe} [nm]	k_{DA}^{-1} [ps], exp. RT	77 K	4.2 K	k_{DA}^{-1} [ps], calc.
Rba. sphaeroides 2.4.1	795/800	800/840	0.7 [1]	1.2 [1]	1.5/1.3 ± 0.2 [1]	
Rba. sphaeroides (M(Y)210)	810	860	0.7 [2]			
Rps. acidophila 10050	810	870	0.9 [2]			
	801		0.8 [3]	1.3 [3]		
	785	870	0.9 ± 0.1 [4]			0.7–1.3 ps [a,5]; 0.91 [6]
Rps. acidophila modif. (ZnBPhe *a*) [8]	785	870	0.8 ± 0.1 [4]			0.8–1.1 ps [a,5]; 0.75 [6]
Rps. acidophila (3-vinyl-BChl *a*) [8]	754	870	1.4 ± 0.2 [4]			1.1–1.5 ps [a,5]; 0.75 [6]
Rps. acidophila (3^1-OH-BChl *a*) [8]	742	870	1.8 ± 0.2 [4]			1.2–1.6 ps [a,5]; 1.34 [6]
Rps. acidophila (3-acetyl-Chl *a*) [8]	685	870	4.4 ± 0.5 [4]			29.1–38.1 ps [a,5]; 13.8 [6]
Rps. acidophila (Chl *a*) [8]	660	870	8.3 ± 0.5 [4]			548–702.8 ps [a,5]; 43.7 [6]
Rsp. molischianum	790	(790–870)	1.2 [7]			1.3 [7]
	800	(790–870)	0.9 [7]			0.8 [7]
	810	(790–870)	1.0 [7]			0.9 [7]
	830	(790–870)	0.5 [7]			0.4 [7]

[a] Stokes shift 80 cm^{-1}–0 cm^{-1}; [1] Pullerits et al., 1997; [2] Kennis et al., 1997; [3] Ma et al., 1997; [4] Herek et al., 2000; [5] Linnanto and Korppi-Tommola, 2002; [6] Scholes and Fleming, 2000; [7] Ihalainen et al., 2001; [8] modified pigment at site B800 (see text)

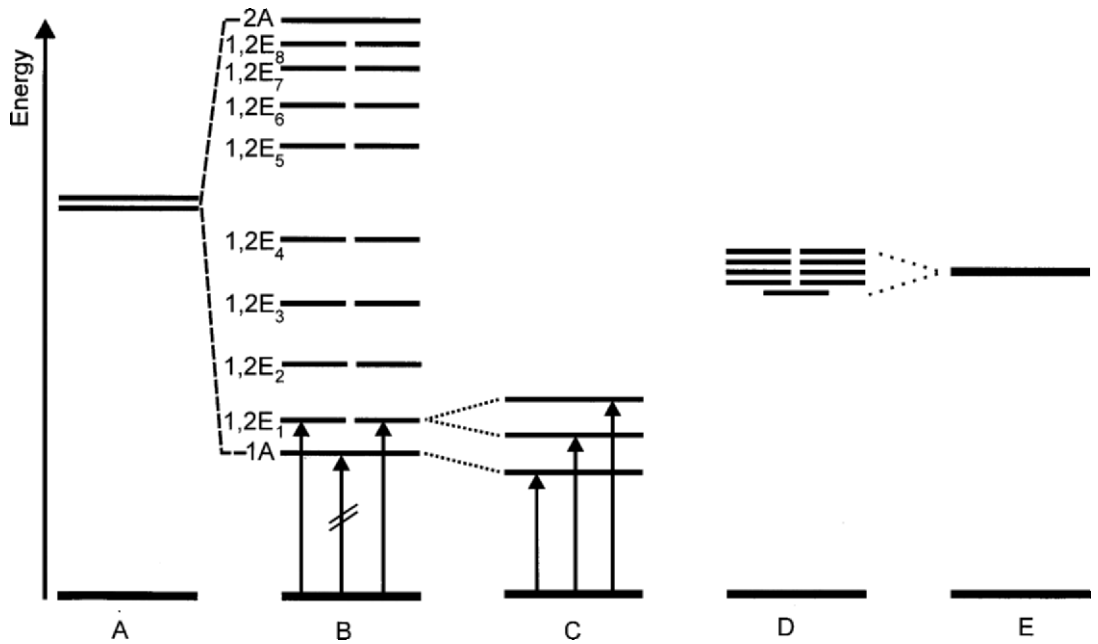

Fig. 1. Schematic representation (not to scale) of the energy level structures of the circular aggregates BChl-B800 (D) and BChl-B850 (B) consisting of 9 weakly and 18 strongly coupled BChls *a,* and of their building blocks, monomeric BChl-'B800' (E) and dimeric BChl-'B850'$_{\alpha,\beta}$ (A). Whereas (B, D) represent the perfect C_9 symmetry, the influence of disorder on the lowest three transitions in BChl-B850 is shown in (C).

Ihalainen et al., 2001) take into account interactions between all BChl in the highly symmetric (C_8, C_9) circular structures (McDermott et al., 1995, Hu et al., 1997). The B800 compartment of *Rps. acidophila* is a ring of 9 BChl *a* molecules with Mg-Mg distances of 21.2 Å and the B850 waterwheel-like compartment is a ring of 18 BChl *a* molecules with alternating distances of 8.9 and 9.6 Å. The closest BChl-BChl distances between the two rings are approximately 18 Å. There are analogous results for *Rsp. molischianum* (Ihalainen et al., 2001), where the 8 BChls *a* and 16 BChls *a* in the respective compartments are separated by somewhat smaller distances, with distinct differences in the orientation of the BChl-B800 transition dipole moments (Koepke et al., 1996).

The B850 Circular Aggregate without Disorder. In LH2 from *Rps. acidophila*, the site energies of BChl-B850$_\alpha$ and BChl-B850$_\beta$ (diagonal elements of the B850-part of the Hamiltonian) were calculated (with explicit inclusion of the binding histidine residues) to 784 nm and 779 nm, respectively (Linnanto et al., 1999). The interaction energies (off-diagonal elements) between neighboring BChl-B850 (calculated by treating them as a supermolecule) amount to 622 cm^{-1} (intra-) and 562 cm^{-1} (inter-subunit). They are larger than those obtained by calculations using point monopole-approximations (Sauer et al., 1996) or the transition density cube approximation (Krueger et al., 1998). The exciton level manifold including also dipole-dipole interactions of non-neighboring BChl-B850 in a perfect circular arrangement, is given in Fig. 1, with each energy level representing a coherent superposition of individual BChl excitations. The optically-allowed transitions terminate in the degenerate 1,2E$_1$ state (main transition at 862 nm) and the 2A-state (weak transition at 719 nm). The dipole moment of the former is enhanced by a factor of about $\sqrt{9}$, compared to monomeric BChl *a,* but the excitation density is identical at all 18 BChl *a*-sites, predicting an (initial) exciton delocalization over the entire ring. The results are remarkable with respect to EET: i) the lowest excited state is 'optically dark' and therefore very long-lived, which strongly reduces competition of radiative processes with EET; ii) excitation into the dominating transition(s) to 1,2E$_1$ renders the energy immediately available at each site of the entire B850 ring; iii) there is a large overall splitting of the energy levels ('exciton splitting') of more than 2000 cm^{-1}, which should accelerate B800-B850 as well as the carotenoid-to-B850 EET (see below and Chapter 30,

Koyama and Kokitani); and, iv) interactions between BChl-B800 and BChl-B850 are very weak.

Considering these predictions that are based on the C_9 symmetry and assuming no disorder, it is interesting to look at some experimental data. B800-depleted LH2 have been studied from *Rba. sphaeroides* (Bandilla, 1995; Bandilla et al., 1998; Koolhaas et al., 1998; Leupold et al., 1999b) and *Rps. acidophila* (Herek et al., 2000). The properties of their 850 nm-bands are almost identical to wild type (WT) complexes; that is, the influence of BChl-B800 is negligible (Bandilla, 1995; Koolhaas et al., 1998; Nowak, 1999; Leupold et al., 1999b; Herek et al., 2000). The B850 bands of both samples show clear indications of disorder (Nowak, 1999; Leupold et al., 2000). Steady state and ultrafast kinetic absorption data indicate an even larger exciton splitting (and/or exciton-vibronic manifold) than calculated, and suggest non-negligible higher-energy transitions of BChl-B850 around 800 nm (Koolhaas et al., 1998; Leupold et al., 1999b; Herek et al., 2000).

The B800 Circular Aggregate without Disorder. Linnanto et al. (1999) calculated a Q_y transition at 797 nm for monomeric BChl-B800 of *Rps. acidophila,* including 9 neighboring amino acid residues, part of the carotenoid and the phytyl chain of the closest BChl-B850. Using a similar approach, Ihalainen et al. (2001) obtained a value of 798 nm for LH2 from *Rsp. molischianum*. These values are considerably red-shifted compared to BChl in any polar solvent (e.g., 786 nm in quinoline; Limantara et al., 1997), suggesting the presence of special pigment-protein interactions like H-bonding to the 3-acetyl-group (Sturgis and Robert, 1996; Hu et al., 2002), steric distortions or axial ligation (Hu et al., 2002); therefore, explicit inclusion of the protein environment in the calculation of the BChl-B800 site energy is essential (Scholes et al., 1999). When applied to LH2 with exchanged B800-pigments (Table 1; Herek et al., 2000), environment-induced red-shifts are observed for all but one substitute pigment (Chl *a*). Assuming that the latter lacks specific protein interactions, its Q_y absorption maximum can be used to determine a refractive index of n = 1.59 at the B800 binding site (Eichwurzel et al., 2000; I. Eichwurzel, unpublished).

Using these Q_y energies as diagonal elements of the B800-part of the Hamiltonian and off-diagonal interaction energies of 30–40 cm^{-1}, as calculated according to the point-dipole model, a (disorder-free) C_9-symmetric B800 energy-level is obtained with only half of the level numbers as for B850, and a much closer spacing (excitonic splitting <100 cm^{-1}) (see Fig. 1). Again, the most intense radiative transition from the ground state is that to the lowest pair of degenerate E levels (λ_{max}=799 nm) (Linnanto et al., 1999).

B800-B850 Interactions. Including BChl *a* interring interactions (≤30 cm^{-1}) reduces excitonic splitting of the Q_y manifold of BChl-B800, while slightly increasing that of neighboring BChl-B850 levels (Linnanto et al., 1999), predicting a small red-shift of B850 in LH2, compared to the BChl-B800 depleted pB850. Experimental results for the disordered systems of native complexes are in agreement with this prediction: namely a red-shift of 2 nm for *Rba. sphaeroides* (Leupold et al., 1999b).

Consequences of Deviations from Highly Symmetric Circular Structures. For a simulation of the optical properties of single LH2 complexes (van Oijen et al., 1999; Chapter 21, Köhler and Aartsma), homogeneous broadening and intra-aggregate disorder have to be considered. Corresponding simulations for LH2 ensembles must additionally include inter-aggregate disorder:

i) Variations of the BChl environment in the circular aggregate may result in a Gaussian distribution of Q_y energies (diagonal disorder) while symmetry is conserved, resulting in non-negligible oscillator strengths in higher — originally forbidden — transitions (among them 1A). The respective absorption bands become increasingly inhomogeneously broadened (Hu et al., 1997).

ii) Variations of BChl *a* positions and orientations along the circular aggregate result in changes of interactions (off-diagonal disorder) and give rise to similar changes, but should be of minor importance (Wu and Small 1997, 1998).

iii) Elliptical deviations from perfect circular arrangements were invoked from low-temperature fluorescence excitation spectra of single LH2 complexes (van Oijen et al., 1999; Chapter 21, Köhler and Aartsma), causing a split of the B850 Q_y-band into two sub-bands (Matsushita et al., 2001; Hu et al., 2002; for an analysis of intra- and inter-aggregate disorder, see Mostovoy and Knoester, 2000).

iv) For 'broken' rings a lift of level degeneracy

would also be expected. In this case, the oscillator strength would not be symmetrically distributed to the two sub-bands (van Oijen et al., 1999).

Experimentally, intra-aggregate disorder is evident for B800: several narrow bands around 800 nm are seen in single-complex spectra of LH2 from *Rps. acidophila* at 1.2 K, while the B850 Q_y band consists (in most cases) of two broad sub-bands of unequal intensities (interpreted as an elliptical deformation, van Oijen et al. 1999; Matsushita et al., 2001; Chapter 21, Köhler and Aartsma). Remarkably, such double-band substructure has also been resolved for ensemble-averaged B850 in LH2 from *Rba. sphaeroides* at room temperature using nonlinear polarization spectroscopy in the frequency domain (NLPF), indicating that intra-aggregate disorder is small (Leupold et al., 2000). This would argue for a relatively uniform degree of ellipticity in the B850 ensemble. There is no such substructure in the C_8-symmetric LH2 of *Rsp. molischianum* (Leupold et al., 2000).

Optical Properties Derived from the LH2 Q_y Exciton Model. To simulate the Q_y absorption and the CD spectrum of LH2, homogeneous broadening has to be considered (Linnanto et al., 1999; Ihalainen et al., 2001). The results obtained for *Rps. acidophila* (Linnanto et al., 1999; Linnanto and Korppi-Tommola, 2000) and for *Rsp. molischianum* (Ihalainen et al., 2001) appear to be promising. In particular, the maxima and shapes of the two Q_y absorption bands as well as the main features of the circular dichroism (CD) spectra are relatively well reproduced. Also well reproduced is the red-shift of the CD zero-crossing with respect to the absorption maximum, and the CD fine structure in the 800 nm region resulting from overlap of B800 and higher excitonic B850 contributions (Bandilla, 1995; Koolhaas et al., 1997; Bandilla et al., 1998).

b. Excitation Energy Transfer B800 → B850

The excitonic energy level systems of BChl-B800 (Donor) and BChl-B850 (Acceptor) have been used to calculate EET rates according to Fermi's Golden Rule (Linnanto and Korppi-Tommola, 2000; Ihalainen et al., 2001). Spectral overlap of D and A exciton states with pump and probe pulses has been considered. For comparison with the experimental rates, the resulting distribution of EET rates is fitted by triple exponentials (Table 1). Remarkably, the calculated EET rates are not lower, but actually somewhat higher than the experimental values. In LH2 from *Rps. acidophila*, the 'dark states' $1,2E_2$, $1,2E_3$ of B850 located in the gap between $3,4E_1$ of B800 and $1,2E_1$ of B850 (Fig. 1), play an essential role. For LH2 of *Rsp. molischianum*, only $1,2E_2$ are in that gap, which is in agreement with the somewhat slower EET (Ihalainen et al., 2001).

Using the same method (CIEM), the effect of exchanging the BChl *a* of the B800 ring by modified pigments (Bandilla, 1995; Bandilla et al. 1998; Fraser et al., 1999) has also been investigated (Linnanto and Korppi-Tommola, 2002). The energetic positions of the shifted 800 nm-absorption bands (Herek et al., 2000) are well reproduced by the calculations, but the calculated EET rates from the modified pigments to BChl-B850 are still too slow (Table 1). The same discrepancy in EET rates was obtained using the transition density cube approach (Scholes and Fleming, 2000), and has been discussed by these authors and also by Linnanto and Korppi-Tommola (2002).

In their Förster-type calculation of EET rates for modified B'800' → BChl-B850, Herek et al. (2000) obtained a perfect qualitative reproduction of the diminished rates after introducing different pigments, but with a constant deviation by a factor of five. These calculations were based on a monomeric Q_y-transition dipole for the acceptor, BChl-B850. From nonlinear absorption measurements, however, the Q_y-transition dipole moment of BChl-B850 has been determined to be ≈ 25 D (Leupold et al., 1996; Stiel et al., 1997), reflecting the high degree of initial exciton delocalization in B850: the transition dipole moment scales with the square root of the pigment number (N_{del}) over which the exciton is delocalized, resulting in $N_{del} = 14 \pm 6$ for LH2 from *Rps. acidophila* (Stiel et al., 1997) and 16 ± 4 for the *Rba. sphaeroides* complex (Leupold et al., 1996). Recently, Book et al. (2000) determined a comparably high initial coherence length for LH2 from *Rba. sphaeroides* ($N_{del} \approx 13$) and asserted that *it is this delocalization length which is relevant to the energy transfer process* (Kimura and Kakitani, 2003). These enhanced transition dipoles would enlarge the EET rates by more than one order of magnitude; that is, the calculated EET would now become even too fast. However, the spatial extent of the charge distribution is non-negligible under these conditions and the point-dipole approximation may not be appropriate for EET modeling (Book et al., 2000). Moreover, the usual assumption of 700 fs for complete excited electronic state-thermalization in

BChl-B800 prior to EET, as a pre-condition for the validity of the Förster-based reasoning, remains to be confirmed (Ma et al., 1997). Results with dissolved BChl *a* (Book et al., 2000) suggest a cautious interpretation; possibly, the theory of intermediate EET (Kimura et al., 2000) is more appropriate for the EET process BChl-B800 → BChl-850.

EET from BChl-B850 of LH2 may occur either to another BChl-B850 or to BChl-B875 of LH1. For the latter process, a time constant of 4.6 ± 0.3 ps has been determined at room temperature in a mutant of *Rba. sphaeroides* lacking the RC. A second time constant of 26.3 ± 1.0 ps has been attributed to excitation migration in the LH2 pool preceding EET to LH1. Back transfer BChl-B875 → BChl-B850 has not been observed (Nagarajan and Parson, 1997). For a single LH2 → LH2 EET step, a calculated value of 10 ps still awaits experimental verification (Hu et al., 2002).

C. The Core Antenna Complex, Light Harvesting Complex 1

For BChl-B870 in LH1 of purple bacteria, a waterwheel-like closed circular arrangement has been assumed, analogous to that of BChl-B850 of LH2; however, it has a larger diameter and binds up to 34 pigments per RC all located in the center of the ring. This model is based on the low-resolution structure of LH1 (Karrasch et al., 1995) and of LH1-RC complexes from strains lacking the PufX protein (Walz et al., 1998). For such BChl arrangements, exciton spectra and dynamics can be expected which are largely comparable to B850. Indeed, the steady state spectroscopic properties of LH1 from *Rsp. rubrum*, in which up to 90% BChl *a* was replaced with Zn-BPhe, could be simulated by altering merely dipole strengths and maintaining nearest-neighbor interactions (400 cm^{-1}) and diagonal disorder (600 cm^{-1}) similar to those of LH2 (Wendling et al., 2002). The recent, somewhat 'spiral-shaped' structure of LH1 in a core complex still awaits theoretical interpretation, but like any deviation this is expected to influence the exciton level structure (Roszak et al., 2003).

A smaller unit size of 20 BChls has been determined for PufX-containing LH1 from *Rba. sphaeroide*s, in which a fraction of the native BChl *a* had been replaced by Ni-BPhe *a,* from 40 fs pump-probe experiments within the 875 nm band (Fiedor et al., 2000); this was also confirmed by fluorescence yield and decay measurements (Fiedor et al., 2001). This relatively small unit size agrees with the suggestion that PufX may interrupt ring formation (Cogdell et al., 1996). Remarkably, substitution of just one out of the twenty BChls *a* by Ni-BPhes is sufficient to induce a monoexponential 60 fs-ground state recovery, by-passing the fluorescent level which in native LH1 is populated within 750 fs after Q_y-excitation (Fiedor et al., 2000). In a similarly substituted LH1-RC system, the EET BChl-B875 → RC would be completely inhibited. Further, a single quencher pigment within a LH1-RC complex, such as a BChl cation radical (Law and Cogdell, 1998), would also suffice to prevent ISC. Varying oligomer sizes up to 10 or 11 αβ-heterodimers in LH1 from the PufX-containing M21 strain of *Rba. sphaeroides,* which lacks LH2, has only a minor effect on the Q_y absorption maximum (Westerhuis et al., 2002).

EET from LH1 to the RC occurs in about 25 ps at RT and, remarkably, the back transfer is about three times faster. Because the initial electron transfer step in the RC occurs in 3 ps, trapping and photoprotection of an already closed RC is efficient (Hu et al., 2002).

III. Excitation Energy Transfer in Light-Harvesting Complex II-type Complexes of Higher Plants

Higher plants possess complex light-harvesting antenna systems for both Photosystems I and II (PS I and PS II). Most abundant is the peripheral LHC II, which binds Chl *a* and *b*, and is associated mainly with PS II. LHC II consists of trimers of closely related proteins, Lhcb1-3, which are members of a large protein family also including the monomeric minor PS II antenna complexes CP29, CP26, CP24 (alternatively designated Lhcb4, Lhcb5 and Lhcb6), as well as Lhca1-4 of PS I, and the Chl *a/c* containing complexes from heterokont algae (Jansson, 1994). Recently the structure of pea PS I including the Lhca1-4 proteins has been solved to 4.4 Å, confirming the proposed structural similarities of these proteins to LHC II and their pairwise, Lhcb1/4 and Lhcb2/3 dimer-formation (Ben-Shem et al., 2003).

The extent of excitonic interactions between Chls and their significance for EET in these LHC is much less clear-cut than for those of purple bacteria: i) the arrangement of the chromophores (Kühlbrandt et al., 1994; Liu et al., 2004; Standfuss et al., 2005) is considerably less symmetric; ii) the previously

available resolution (3.4 Å) could not distinguish between Chls *a* or *b* (Kühlbrandt et al., 1994). An assignment, based on an assumed necessity of triplet quenching by the two central luteins (Kühlbrandt et al., 1994), was only partly verified by mutagenesis (Bassi et al., 1999; Remelli et al., 1999; Rogl and Kühlbrandt, 1999; Rogl et al., 2002; Chapter 26, Paulsen). As a further complication, promiscuous binding sites (occupied by Chl *a* or *b*) have been proposed (Bassi et al., 1999; Remelli et al., 1999; reviewed by van Amerongen and van Grondelle, 2001; but see also Rogl and Kühlbrandt, 1999; Rogl et al., 2002); iii) orientations of the Chl transition dipole moments remained unresolved in the 3.4 Å Kühlbrandt-model; and, iv) neither the site energies of the individual and/or coupled pigments are known, nor the refractive index of the pigment-surrounding medium at the respective binding sites (see below). Hence, calculations of excitonic interactions as well as EET rates between pigments have been controversial (Kühlbrandt et al., 1994; Voigt et al., 1996; Trinkunas et al., 1997; Gradinaru et al., 1998; Renger and May, 2000; Iseri and Gülen, 2001; van Amerongen and van Grondelle, 2001).

Excited state kinetics in LHC II are multiphasic with lifetimes ranging from a few 100 fs to several ns (Eads et al., 1989; Palsson et al., 1994; Bittner et al., 1994, 1995; Kleima et al., 1997; Gradinaru et al., 1998; summarized in Table 2). The fastest EET step (about 200 fs) occurs from Chl *b* to Chl *a* within the monomeric subunits (Kleima et al., 1997), but it has not yet been established whether its nature is excitonic or incoherent hopping-type (Leupold et al., 1999a). Close packing of the pigments and recent nonlinear laser-spectroscopic studies (Krikunova et al., 2002; Leupold et al., 2002; Schubert et al., 2002; Voigt et al., 2002) render strong excitonic interactions among certain Chls in LHC II and related complexes highly likely, but their extent is still controversial, as well as any consequences thereof for EET.

Most work on EET has been interpreted in the framework of the Förster-formalism. Simulations of ultrafast transient absorption in CP29 did not agree with the experimental data. Instantaneous bleaching in the spectral region of the pumped Chl *b* (640 nm) and, *simultaneously* of Chl *a*, can not be explained by Förster-type EET (Cinque et al., 2000). The ultrafast EET steps, observed in one- and two-color pump and probe experiments (Bittner et al., 1994, 1995), are now explained by excitonically coupled Chl *a/b* heterodimers (Renger and May, 2000).

Table 2. Experimentally observed EET time constants (in ps) in LHC II and CP29 (adapted from Gradinaru et al., 1998)

λ_{pump} [nm]	λ_{probe} [nm]	LHC II	CP29
640	678	0.3; 1	0.35
650	670–676	≤0.2, 0.5, 2–6	2.2
660–670	670–680	0.3–0.4	0.3
670	678	10–20	10–13

An early exciton calculation concluded that the lowest excited state in LHC II carries almost no excitonic character (Voigt et al., 1996): the calculated dipole strength was only 1.16 times that of monomeric Chl *a*, whereas that of the next higher state was twice as strong. Trinkunas et al. (1997) were able to model, by the Förster-formalism, the transient absorption data of Connelly et al. (1997) as well as steady state spectroscopic data obtained with LHC II. The latter was only possible if two Chl *a* (a1 and a2; Kühlbrandt et al., 1994) were swapped for Chl *b* (which is not in agreement with mutagenesis studies). More recently, it has been shown theoretically that the lowest excited state has significant excitonic character but with a dipole strength only 0.5 times that of Chl *a* (Renger and May, 2000). A somewhat larger value (0.8) was derived from hole-burning experiments (Pieper et al., 1999). Van Amerongen and van Grondelle (2001) used the pigment assignment of Remelli et al. (1999) to calculate excitonic interactions and EET rates, concluding that the lowest excited state is essentially localized on a single Chl *a*. Such a value (1.18) was corroborated in a study of super-radiance (Palacios et al., 2002). However, exciton delocalization is expected to be strongly time-dependent (Dahlbohm et al., 2001), and steady-state super-radiance measurements may yield only the final value after thermalization. From a two-pulse photon echo study it was also concluded that the long wavelength Chls *a* in LHC II are only weakly coupled (Hillmann et al., 2001).

Early experimental indications for strong excitonic interactions in LHC II and related complexes are based on the high optical activity (Ide et al., 1987; Hemelrijk et al., 1992). However, distortions of the Chl macrocycle may also lead to strong CD (Wolf and Scheer, 1973).

Recent non-linear absorption and intensity-dependent NLPF work favors strong excitonic interactions in LHC II: Both experiments indicated that a spectral form emitting at 682 nm has a dipole strength twice that of monomeric Chl *a* (Schubert et al., 2002).

The most obvious explanation for the enhancement is excitonic interaction between the Chl molecules forming the terminal emitter. These experiments could not distinguish between a homo- (Chl *a*/Chl *a*) or a hetero-dimer (Chl *b*/Chl *a*). A special variant of the NLPF-technique was employed to assess heterodimeric interactions in LHC II (Krikunova et al., 2002). NLPF-spectra are pumped in a low-energetic band, and probed in a (spectrally well separated) higher-energetic absorption band. Remarkably, Chl *a* excitation in the Q_y region resulted in a NLPF-response in the higher-energy Chl *b*-Soret-region, which appears to be explained only by strong excitonic coupling between certain Chls *a* and *b*. Strong Chl *a/b* interactions were also inferred from NLPF experiments with the structurally-related antenna complex, CP29 (Voigt et al., 2002). There are, nonetheless, marked differences between both complexes: whereas in LHC II the lowest energy Chl *a* (~678 nm) appears to be strongly coupled to Chl *b*, the red-most Chl-form in CP29 was attributed to a non-coupled Chl *a* (Pieper et al., 1999; Voigt et al., 2002). The strongly interacting pigments in CP29 appear to be a Chl *a* absorbing at 670 nm and a Chl *b* absorbing at 640 nm. These observations are consistent with the assignment of the longest wavelength band in LHC II to Chl a2 (Remelli et al., 1999; Rogl and Kühlbrandt, 1999; Rogl et al., 2002): Chl a2 is closest to Chl 'b2' at a binding site which is apparently lacking in CP29. The different character of the lowest-energy transition in LHC II and CP29 is corroborated by studies both at low (Pieper et al., 1999) and ambient temperatures (Leupold et al., 2002). Stepwise two-photon excitation with 100-fs pulses in the Q_y-region of Chl *a* and *b* elicits a weak 'blue' fluorescence of considerably different character (Leupold et al., 2002). The blue emission profiles of LHC II are virtually identical (peaking at about 475 nm) when exciting in the Chl *a* (680 nm) or Chl *b* (650 nm) range: this is consistent with strong Chl *a*/*b* coupling. By contrast, two different peaks are observed in CP29 upon excitation of Chl *a* (at 450 nm) and Chl *b* (at 475 nm).

From the above results and previous site-directed mutagenesis studies on LHC II (Remelli et al., 1999; Rogl and Kühlbrandt, 1999; Rogl et al., 2002), we suggested that Chl a2 (Kühlbrandt et al., 1994) is involved in the proposed excitonic pigment cluster (Fig. 2) (Schubert et al., 2002). The distance to the nearby Chl 'b2' (8 Å) was the closest of all mutual Chl-Chl distances determined in pea LHC II (Kühlbrandt et al., 1994).

Very recently the structure of spinach LHC II was solved by X-ray crystallography to <3 Å (Liu et al., 2004; Standfuss et al., 2005). The considerably refined structure confirmed many previously observed features (Kühlbrandt et al., 1994) but also revealed important hitherto unknown details: Two additional Chls (Chls *b* 601 and 605, in the nomenclature of Liu et al., 2004) were detected. All Chls *a* and *b* could be identified directly. Thus, two 'Chls *b*' (previously

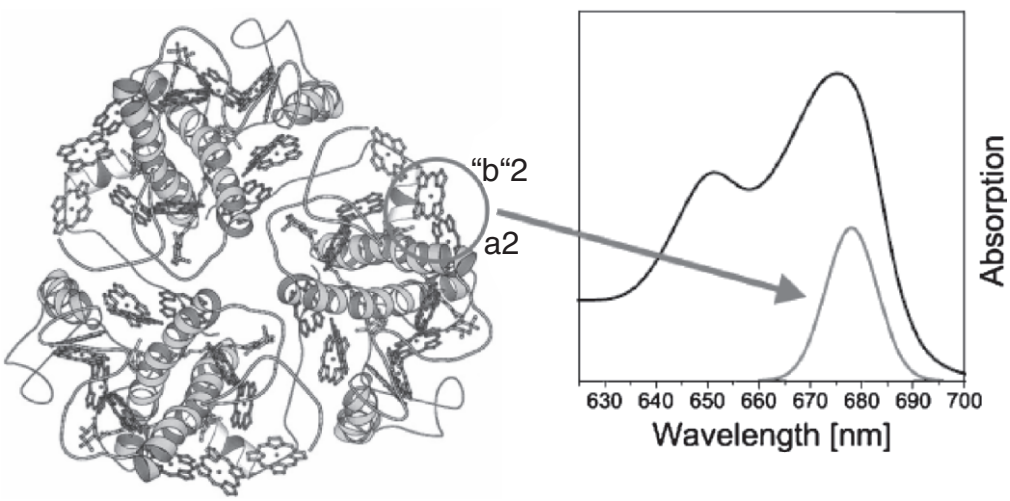

Fig. 2. Structure (left, adapted from Rogl et al., 2002) and absorption spectrum (solid line, right) of LHC II. The red-most excitonic transition (peaking at 678 nm, dashed line, right) can be assigned to a cluster involving the pigment binding sites a2 and 'b'2 in the structural model of LHC II (but compare also the recent, refined structures of Liu et al., 2004; Standfuss et al., 2005). See also Color Plate 7.

designated b2, now: 611 and b3 now: 614) had to be re-assigned as Chl *a*. One 'Chl *a*' (a7 now: 607) had to be swapped for Chl *b*. No indication of promiscuity of the binding sites was found. Orientations of the transition dipole moments of all Chl were identified. Thus, more reliable estimates of excitonic interactions strength between individual pigments could be given (Liu et al., 2004; see supplementary information): Strong excitonic coupling is inferred for Chl *a* 611/612 (a2/'b2') as well as at least two Chl *a/b*-pairs: Chl *a* 604 (a6)/*b* 611 (b6) and Chl *a* 603 (a5)/*b* 609 (b5). Thus, our predictions, from nonlinear laser-spectroscopic studies on excitonic interactions between Chls *a* and *a* as well as Chls *a* and *b* in LHC II, are confirmed by the structural data of Liu et al. (2004). Based on this refined, atomic level structure of LHC II much deeper insight into light harvesting in plants can be expected for the near future.

The Chl *a* 611/612 (a2/'b2') pair (possibly involving interactions with further nearby pigments), is located on the outer surface of LHC II, also in its trimeric form (Fig. 2). Its red-shifted absorption renders it a 'relay state' (for EET to neighboring complexes) of LHC II. Additionally, the enhanced dipole moment may 'attract' excitations from inside the complex to the surface. This would contribute to the efficiency of light-harvesting in an extended PS II antenna-network, because Chl a2 are the most closely spaced pigments in adjacent LHC II trimers.

IV. Excitation Energy Transfer in Chlorosomes

Chlorosomes occur in both green filamentous- (designated F-chlorosomes) and green sulfur-bacteria (S-chlorosomes). Among LHCs, these extremely large, extra-membranous structures are unique and their function, almost exclusively, appears to result from pigment-pigment interactions: the protein content of chlorosomes is generally very low (Olsen, 1998), and chlorosomes devoid of any protein exhibit nearly the same spectroscopic properties as those containing protein. However, the CD spectra of such isolates are quite variable (Griebenow and Holzwarth, 1989) and proteases induce distinct changes (Niedermeier et al., 1992); the function of the remaining proteins is therefore still unclear (Chapters 15, Frigaard et al., and 20, de Boer and de Groot). Chlorosomes consist of a core and an envelope. The core contains several thousand molecules of BChl *c, d* or *e* (depending on the species), which are organized in 10–30 (but see also Niedermeier et al., 1992) parallel tubular structures called rod elements (Blankenship et al., 1995; Olsen, 1998). Rod diameters and lengths are about 5 nm and 100 nm, respectively, for F-chlorosomes, or 10 nm and 180 nm, respectively, for S-chlorosomes (Olsen, 1998).

BChls within the rods are strongly excitonically coupled, but there is also non-negligible nearest-neighbor inter-rod interaction. Otherwise, a spectroscopic behavior would be expected that is comparable to that of the well-known J-aggregates (Buck and Struve, 1996; Bednarz and Knoester, 2001), with most of the dipole strength concentrated in the lowest transition. This, however, is not the case with chlorosomes: absorption spectra, the large Stokes-shift of fluorescence and hole-burning spectra all indicate that the lowest exciton band carries only a few percent of the total dipole strength of the Q_y transition, while transitions to higher exciton levels are strongly allowed. From pump-probe (Savikhin et al., 1998a) and temperature-dependent fluorescence spectra (Mauring et al., 1999), a tubular aggregate model has been developed for F-chlorosomes. The unit BChl *c* building block comprises 24 strongly coupled BChls *c*, arranged in six parallel chains of four BChls *c*: the maximum inter-chain interaction of 44 cm^{-1} is equal to about one tenth of intra-chain nearest-neighbor interaction energy (Yakovlev et al., 2002). For comparison, a cluster size of 16 BChls *c* has been derived from the EPR line width of partly oxidized F-chlorosomes (van Noort et al., 1997). The individual exciton wave functions are delocalized over 7–12 BChl *c* molecules, and the coherence size of the steady state exciton wave packet is 7.4 BChl *c* (Yakovlev et al., 2002; for definitions, see Fidder et al., 1991; Meier et al., 1997). Much larger delocalization lengths have been recently reported by Holzwarth and Prokhorenko (2002). Their model (Holzwarth and Schaffner, 1994; Prokhorenko et al., 2000; Chapter 20, de Boer and de Groot) has a higher pigment packing density (36 chains per rod of S-chlorosomes of *Chlorobium (Chl.) tepidum*) than the model of Yakovlev et al. (2002), resulting in high intra-stack (-chain) as well as inter-stack interaction energies (about 500 cm^{-1} and 200 cm^{-1}, respectively).

F-chlorosomes are attached to the cytoplasmic membrane via a baseplate containing monomeric BChl *a* (B795) which is essential for EET to the RC. Within the Q_y-band of F-chlorosomes, relaxation from

the high-energy exciton levels is multiphasic with times between sub-ps to several ps, probably reflecting faster intra-rod processes and slower inter-rod exchange. These processes are temperature-dependent, as is the final step from the lowest BChl *c* Q_y exciton-level to the base plate BChl *a*, which takes about 50 ps at low temperatures and 10–20 ps at RT (Prokhorenko et al., 2000 and references therein).

EET from S-chlorosomes to the RC also occurs via a base plate; however, these EET kinetics are dependent not only on temperature but also on redox potential. At high (positive) redox potential, the chlorosomal Q_y lifetime is shortened and EET to the base plate BChl *a* is strongly reduced. A similar redox dependence has been observed for the subsequent EET steps in green sulfur bacteria, thereby shortening, for example, the Q_y lifetime in the FMO complex (see reviews by Olsen, 1998 and Psencik et al., 1998)

V. Excitation Energy Transfer in the Fenna-Matthews-Olsen (FMO) Complex

The FMO complex of green sulfur bacteria is a trimeric, water-soluble pigment-protein complex carrying 7 BChl *a* in each monomeric subunit. In the EET chain, it links the chlorosome and the RC. The spatial arrangement of the 7 BChl *a* in the monomer, and the mode of their attachment to the protein matrix, are known at a resolution of 1.9 Å (Fenna and Matthews, 1975; Tronrud and Matthews, 1993; Li et al., 1997). Yet, only recently has a detailed picture of the structure-function relationship emerged. Both pigment-pigment and pigment-protein interactions contribute to the absorption band substructure and EET processes and, in particular, the latter are theoretically not well understood (Pearlstein, 1992; Savikhin et al., 1998b, 1999). The 7 BChl *a* in the monomeric subunit are 'irregularly' arranged (as in LHC II), with nearest neighbor Mg-Mg distances between 11 and 15 Å. Therefore, significant transition-dipole interaction can be expected, as reflected by a redistribution of oscillator strengths and energetic shifts of the 7 Q_y transitions of the BChls at the seven different sites and, also, by large CD signals (Savikhin et al., 1998b, 1999). The closest distance between BChls in different subunits of the trimer is about 24 Å, the maximum inter-monomer coupling strengths (10–20 cm^{-1}, depending on the model) are about one order of magnitude smaller than intra-monomer couplings (100–190 cm^{-1}) (Pearlstein, 1992; Vulto et al., 1998a; Iseri and Gülen, 1999; Wendling et al., 2002). It is expected, therefore, and largely confirmed, that the essential FMO structure-function relations are dominated by the properties of the monomer.

At room temperature, neither the Q_y-absorption (λ_{max} = 809 nm) nor the CD show fine structure. They become well-structured, however, at 77 K: Philipson and Sauer (1972) resolved 5 bands for FMO from *Prostecochloris (Ptc.) aestuarii*. Hole-burning studies at temperatures of a few K gave 8 excitonic components (Johnson and Small, 1991), which is one component more than expected for pure intra-monomer BChl interaction and strict C_3-symmetry with identical micro-environments for corresponding BChl sites in all three subunits. A further component has been resolved and the three lowest-energy components have been attributed to the lowest Q_y states in each of the three non-equivalent monomers (Rätsep et al., 1999). These data have been complemented by absorption, linear dichroism, CD and transient spectra (Savikhin et al., 1998b, 1999; Vulto et al., 1998a; Wendling et al., 2002)

Earlier simulations of the Q_y structure of FMO trimers from *Ptc. aestuarii* resulted in seven groups of exciton levels in the range between 775 and 825 nm (Pearlstein, 1992; Lu and Pearlstein, 1993). In each group, the excitation density is distributed (unevenly) over several BChls, but mostly localized at one or two sites ('mini-excitons'). Refined calculations reproduced distinctly different spectral characteristics between FMO from *Chl. tepidum* and *Ptc. aestuari*, in spite of largely identical pigment arrangements (Gülen, 1996; Louwe et al., 1997, Vulto et al., 1998a,b). Calculations have concentrated on monomers, yielding, consequently, seven exciton levels. They suggest, that spectral differences are due to different energies of the BChls at the seven binding sites, possibly related to differences in hydrogen bonding and planarity of the porphyrin rings (Vulto et al., 1998a,b). Unfortunately, these site energies are adjustable parameters in the calculations. They are, currently, neither available experimentally nor from quantum chemical calculations which take into account the protein micro-environment (the latter, however, has been obtained for BChl-B800 in LH2; Linnanto et al., 1999; see above). Other refinements, for example, the inclusion of broadening mechanisms, are already available and have given additional evidence for inter-monomer interactions (Wendling et al., 2002).

There seems to be consensus that after excitation to the highest exciton level, energy relaxation to the

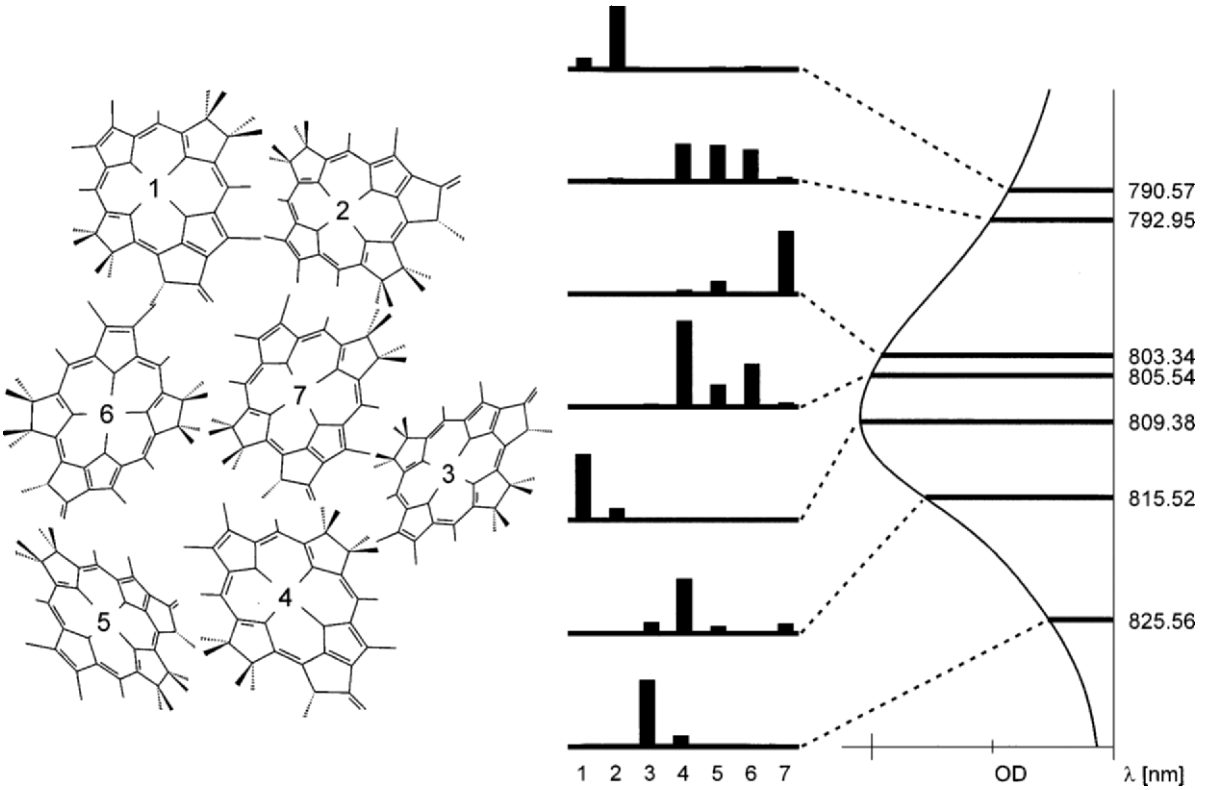

Fig. 3. Simplified projection of the BChl *a*-arrangement in the monomeric subunit of the FMO-complex (left). Room temperature absorption spectrum of the FMO-complex (Q_y-range, right). Exciton levels and corresponding excitation densities at the seven pigment sites (center) are adapted from Vulto et al. (1998a).

second-highest level in several tens of fs is the fastest process in a, possibly branching, cascade down to the lowest level, with time constants gradually increasing up to few ps (Savikhin et al., 1998b, 1999; van Amerongen et al., 2000). As the exciton levels in the relaxation cascade can be linked to defined pigment sites (mini-excitons), the fs/ps time course of EET can be represented in the structural picture as rapidly varying excitations of defined BChls (see Fig. 3 for a preliminary representation). There is an emerging consensus that the final site, preceding EET to the RC, is a BChl in the core of the subunit (site 3) (Vulto et al., 1998a; Owen and Hoff, 2001; Wendling et al., 2002).

Note Added in Proof

Recent experimental results with LH2 of purple bacteria highlight the contribution of exciton transitions to the 'blue absorbance tail' (at around 800 nm) of B850: Hole-burned absorption and line-narrowed fluorescence spectra at 5 K indicate that in *Rba. sphaeroides* more than 2/3 of this 'blue absorbance tail' are of excitonic nature, only the remainder belongs to dysfunctional BChl *a* (Rätsep et al., 2005). Whereas the exciton structure of the blue tail is interpreted by the authors as result of off-diagonal disorder, single-molecule spectroscopy (at 1.4 K) of B850 from *Rps. acidophila* led to the conclusion, that random and correlated diagonal disorder — rather than off-diagonal — dominates (Hofmann et al., 2004).

Structural features of LHC II (Liu et al., 2004) were confirmed at even higher (2.5 Å) resolution (Standfuss et al., 2005). The 2.72 Å data were used to generate a sophisticated excitonic model of EET in LHC II (Novoderezhkin et al., 2005) confirming the predicted excitonic clusters and their relevance for inter-complex EET.

FMO of *Chl. tepidum* was studied by femtosecond two-dimensional heterodyne-detected three-pulse photon echo spectroscopy at 77 K (Brixner et al., 2005). The theoretical analysis revealed the following non-cascading energy relaxation pathways between

the 7 excitonic levels (see also Fig. 3): 7→3→2→1; 6→5 and from level 5 two parallel channels (→4→2→1 and →2→1).

Acknowledgments

The authors gratefully acknowledge support by the Deutsche Forschungsgemeinschaft: SFB 429 TP A2, D.L. and H.L.; and SFB 533 TPA6, H.S.).

References

Bandilla M (1995) Rekonstruktion der Antennen B875 und B850 aus *Rhodobacter sphaeroides* 2.4.1. mit Eintausch chemisch modifizierter (Bacterio-)Chlorophylle. PhD Thesis, University of Munich

Bandilla M, Ücker B, Ram M, Simonin I, Gelhaye E, McDermott G, Cogdell RJ and Scheer H (1998) Reconstitution of the B800 bacteriochlorophylls in the peripheral light harvesting complex B800-850 of *Rhodobacter sphaeroides* 2.4.1 with BChl *a* and modified (bacterio-)chlorophylls. Biochim Biophys Acta 1364: 390–402

Bassi R, Croce R, Cugini D and Sandona D (1999) Mutational analysis of a higher plant antenna protein provides identification of chromophores bound into multiple sites. Proc Natl Acad Sci USA 96: 10056–10061

Bednarz M and Knoester J (2001) The linear absorption and pump-probe spectra of cylindrical molecular aggregates. J Phys Chem B 105: 12913–12923

Ben-Shem A, Frolow F and Nelson N (2003) Crystal structure of plant Photosystem I. Nature 426: 630–635

Bittner T, Irrgang KD, Renger G and Wasielewski MR (1994) Ultrafast excitation energy transfer and exciton-exciton annihilation processes in isolated light harvesting complexes of Photosystem II (LHC II) from spinach. J Phys Chem 98: 11821–11826

Bittner T, Wiederrecht GP, Irrgang KD, Renger G and Wasielewski MR (1995) Femtosecond transient absorption spectroscopy on the light-harvesting Chl *a/b* protein complex of PS II at room temperature and 12 K. Chem Phys 194: 311–322

Blankenship RE, Olsen JM and Miller M (1995) Antenna complexes from green photosynthetic bacteria. In: Blankenship RE, Madigan MT and Bauer CE (eds) Anoxygenic Photosynthetic Bacteria, pp 297–313. Kluwer Academic Publishers, Dordrecht

Book, LD, Ostafin AE, Ponomarenko N, Norris, JR and Scherer NF (2000) Exciton delocalization and initial dephasing dynamics of purple bacteria LH2. J Phys Chem B 104: 8295–8307

Brixner T, Stenger J, Vaswani HM, Cho M, Blankenship RE and Fleming GR (2005) Two-dimensional spectroscopy of electronic couplings in photosynthesis. Nature 434: 625–628

Buck DR and Struve WS (1996) Tubular exciton models for BChl *c* antennae in chlorosomes from green photosynthetic bacteria. Photosynth Res 48: 367–377

Cinque G, Croce R, Holzwarth A and Bassi R (2000) Energy transfer among CP29 chlorophylls: Calculated Förster rates and experimental transient absorption at room temperature. Biophys J 79: 1706–1717

Cogdell RJ, Fyfe PK, Barrett SJ, Prince SM, Freer AA, Isaacs NW, McGlynn P and Hunter CN (1996) The purple bacterial photosynthetic unit. Photosynth Res 48: 55–63

Connelly JP, Müller MG, Hucke M, Gatzen G, Mullineaux CW, Ruban AV, Horton P and Holzwarth AR (1997) Ultrafast spectroscopy of trimeric light-harvesting complex II from higher plants. J Phys Chem B 101: 1902–1909

Cory MG, Zerner MC, Hu X and Schulten K (1998) Electronic excitations in aggregates of bacteriochlorophylls. J Phys Chem B 102: 7640–7650

Dahlbohm M, Pullerits T, Mukamel S and Sundström V (2001) Exciton delocalization in the B850 light-harvesting complex: Comparison of different measures. J Phys Chem B 105: 5515–5524

Damjanovic A, Kosztin I, Kleinekathöfer U and Schulten K (2002) Excitons in a photosynthetic light-harvesting system: A combined molecular dynamics, quantum chemistry, and polaron model study. Phys Rev E 65 art. no. 031919

Eads DD, Castner EW, Alberte RS, Mets L and Fleming GR (1989) Direct observation of energy transfer in a photosynthetic membrane: Chlorophyll *b* to chlorophyll *a* transfer in LHC. J Phys Chem B 93: 8271–8275

Eichwurzel I, Stiel H, Teuchner K, Leupold D, Scheer H and Scherz A (2000) Photophysical consequences of coupling bacteriochlorophyll *a* with serine and its resulting solubility in water. Photochem Photobiol 72: 204–209

Fenna RE and Matthews BW (1975) Chlorophyll arrangements in a bacteriochlorophyll-protein from *Chlorobium limicola*. Nature 258: 573–577

Fidder H, Knoester J and Wiersma DA (1991) Optical properties of disordered molecular aggregates: A numerical study. Phys Rev E 95: 7880–7890

Fiedor L, Scheer H, Hunter CN, Tschirschwitz F, Voigt B, Ehlert J, Nibbering E, Leupold D and Elsaesser T (2000) Introduction of a 60 fs deactivation channel in the photosynthetic antenna LH1 by Ni-bacteriopheophytin *a*. Chem Phys Lett 319: 145–152

Fiedor L, Leupold D, Teuchner K, Voigt B, Hunter CN, Scherz A and Scheer H (2001) Excitation trap approach to analyze size and pigment-pigment coupling: Reconstitution of LH1 antenna of *Rhodobacter sphaeroides* with Ni-substituted bacteriochlorophyll. Biochemistry 40: 3737–3747

Fraser NJ, Dominy PJ, Ücker B, Simonin I, Scheer H and Cogdell RJ (1999) Selective release, removal and reconstitution of Bchl *a* molecules into the B800 sites of LH2 complexes from *Rhodopseudomonas acidophila* 10050. Biochemistry 38: 9684–9692

Georgakopoulou S, Frese RN, Johnson E, Koolhaas C, Cogdell RJ, van Grondelle R and van der Zwan G (2002) Absorption and CD spectroscopy and modeling of various LH2 complexes from purple bacteria. Biophys J 82: 2184–2197

Gradinaru CC, Özdemir S, Gülen D, van Stokkum IHM, van Grondelle R and van Amerongen H (1998) The flow of excitation energy in LHC II monomers: Implications for the structural model of the major plant antenna. Biophys J 75: 3064–3077

Griebenow K and Holzwarth AR (1989) Pigment organization and energy transfer in green bacteria. 1. Isolation of native chlorosomes free of bound bacteriochlorophyll *a* from *Chloroflexus aurantiacus* by gel-electrophoretic filtration. Biochim Biophys Acta 973: 235–240

Gülen D (1996) Interpretation of the excited-state structure of the Fenna-Matthews-Olsen pigment protein complex of *Prosthecochloris aestuarii* based on the simultaneous simulation of the 4K absorption, linear dichroism, and singlet-triplet absorption difference spectra: A possible excitonic explanation? J Phys Chem 100: 17683–17689

Hemelrijk PW, Kwa SLS, van Grondelle R and Dekker JP (1992) Spectroscopic properties of LHCII, the main light-harvesting chlorophyll *a/b* protein complex from chloroplast membranes. Biochim Biophys Acta 1098: 159–166

Herek JL, Fraser NJ, Pullerits T, Martinsson P, Polivka T, Scheer H, Cogdell RJ and Sundström V (2000) B800→B850 energy transfer mechanism in bacterial LH2 complexes investigated by B800 pigment exchange. Biophys J 78: 2590–2596

Hillmann F, Voigt J, Redlin H, Irrgang KD and Renger G (2001) Optical dephasing in the light-harvesting complex II: A two-pulse photon echo study. J Phys Chem B 105: 8607–8615

Hofmann C, Aartsma TJ and Köhler J (2004) Energetic disorder and the B850-exciton states of individual light-harvesting 2 complexes from *Rhodopseudomonas acidophila*. Chem Phys Lett 395: 373–378

Holzwarth AR and Prokhorenko V (2002) Exciton coupling and dynamics in chlorosomes and artificial aggregates. Book of Abstracts, ESF Workshop 'Femtochemistry and Femtobiology', Belek-Antalya, Turkey, 2002

Holzwarth AR and Schaffner K (1994) On the structure of bacteriochlorophyll molecular aggregates in the chlorosomes of green bacteria. A molecular modeling study. Photosynth Res 41: 225–233

Hu X, Ritz T, Damjanovic and Schulten K (1997) Pigment organization and transfer of electronic excitation in the photosynthetic unit of purple bacteria. J Phys Chem B 101: 3854–3871

Hu X, Ritz T, Damjanovic A and Autenrieth F (2002) Photosynthetic apparatus of purple bacteria. Quart Rev Biophys 35: 1–62

Ide JP, Klug DR, Kühlbrandt W, Giorgi LB and Porter G (1987) The state of detergent solubilized light-harvesting chlorophyll *a/b* protein complex as monitoed by picosecond time-resolved fluorescence and circular dichroism. Biochim Biophys Acta 893: 349–364

Ihalainen JA, Linnanto J, Myllyperkiö P, van Stokkum IHM, Ücker B, Scheer H and Korppi-Tommola JEI (2001) Energy transfer in LH2 of *Rhodospirillum molischianum,* studied by subpicosecond spectroscopy and configuration interaction exciton calculations. J Phys Chem B 105: 9849–9856

Iseri EI and Gülen D (1999) Electronic excited states and excitation transfer kinetics in the Fenna-Matthews-Olson protein of the photosynthetic bacterium *Prosthecochloris aestuarii* at low temperatures. Eur Biophys J Biophys Lett 28: 243–253

Iseri EI and Gülen D (2001) Chlorophyll transition dipole moment orientations and pathways for flow of excitation energy among the chlorophylls of the major plant antenna, LHCII. Eur Biophys J 30: 344–353

Jansson S (1994) The light-harvesting chlorophyll *a/b*-binding proteins. Biochim Biophys Acta 1184: 1–19

Johnson SG and Small GJ (1991) Excited-state structure and energy-transfer dynamics of the bacteriochlorophyll *a* antenna complex from *Prostheocochloris aestuarii.* J Phys Chem 95: 471–479

Jungas C, Rangk J, Rigaud J, Joliot P and Vermeglio A (1999) Supramolecular organization of the photosynthetic apparatus of *Rhodobacter sphaeroides*. EMBO J 18: 534–542

Karrasch S, Bullough PA and Gosh R (1995) The 8.5 Angstrom projection map of the light-harvesting complex 1 from *Rhodospirillum rubrum* reveals a ring composed of 16 subunits. EMBO J 14: 631–638

Kennis JTM, Streltsov AM, Vulto SIE, Aartsma TJ, Nozawa T and Amesz J (1997) Femtosecond dynamics in isolated LH2 complexes of various species of purple bacteria. J Phys Chem B 101: 7827–7834

Kimura A and Kakitani T (2003) Theory of excitation energy transfer in the intermediate coupling case of clusters. J Phys Chem B 107: 14486–14499

Kimura A, Kakitani T and Yamato T (2000) Theory of excitation energy transfer in the intermediate coupling case. II. Criterion for intermediate coupling excitation energy transfer mechanism and application to the photosynthetic antenna system. J Phys Chem B 104: 9276–9287

Kleima FJ, Gradinaru CC, Calkoen F, van Stokkum IHM, van Grondelle R and van Amerongen H (1997) Energy transfer in LHCII monomers at 77 K studied by sub-picosecond transient absorption spectroscopy. Biochemistry 36: 15262–15268

Knox RS and van Amerongen H (2002) Refractive index dependence of the Förster resonance excitation transfer rate. J Phys Chem B 106: 5289–5293

Koepke J, Hu X, Muenke C, Schulten K and Michel H (1996) The crystal structure of the light harvesting complex II (B800-850) from *Rhodospirillum molischianum*. Structure 4: 581–597

Koolhaas MHC, van der Zwan G, Frese RN and van Grondelle R (1997) Red shift of the zero crossing in the CD spectra of the LH2 antenna complex of *Rhodopseudomonas acidophila*: A structure based study. J Phys Chem B 101: 7262–7270

Koolhaas MHC, Frese RN, Fowler GJS, Bibby TS, Georgakopoulou S, van der Zwan G, Hunter CN and van Grondelle R (1998) Identification of the upper exciton component of the B850 bacteriochlorophylls of the LH2 antenna complex, using a B800-free mutant of *Rhodobacter sphaeroides*. Biochemistry 37: 4693–4698

Krikunova M, Voigt B and Lokstein H (2002) Direct evidence for excitonically coupled chlorophylls *a* and *b* in LHC II of higher plants by non-linear polarization spectroscopy in the frequency domain. Biochim Biophys Acta 1556: 1–5

Krueger BP, Scholes GD and Fleming GR (1998) Calculation of coupling and energy-transfer pathways between the pigments of LH2 by the ab initio transition density cube method. J Phys Chem B 102: 5378–5386

Kühlbrandt W, Wang DN and Fujiyoshi Y (1994) Atomic model of plant light-harvesting complex by electron crystallography. Nature 367: 614–621

Law CJ and Cogdell RJ (1998) The effect of chemical oxidation on the fluorescence of the LH1 (B880) complex from the purple bacterium *Rhodobium marinum*. FEBS Lett 432: 27–30

Leupold D, Stiel H, Teuchner K, Nowak F, Sandner W, Ücker B and Scheer H (1996) Size enhancement of transition dipoles to one-and two-exciton bands in a photosynthetic antenna. Phys Rev Lett 77: 4675–4677

Leupold D, Lokstein H and Hoffmann P (1999a) Structure-function relationships in the higher plant photosynthetic antenna complex LHC II as revealed by non-linear laser spectroscopy—the problem of 'chlorophyll forms.' Trends Photochem Photobiol 6: 43–52

Leupold D, Stiel H, Ehlert J, Nowak F, Teuchner K, Voigt B,

Bandilla M, Uecker B and Scheer H (1999b) Photophysical characterization of the B800-depleted light harvesting complex B850 of *Rhodobacter sphaeroides*. Implications to the ultrafast energy transfer 800 → 850 nm. Chem Phys Lett 301: 537–545

Leupold D, Voigt B, Beenken W and Stiel H (2000) Pigment-protein architecture in the light-harvesting antenna complexes of purple bacteria: Does the crystal structure reflect the native pigment-protein arrangement? FEBS Lett 480: 73–78

Leupold D, Teuchner K, Ehlert J, Irrgang K-D and Lokstein H (2002) Two-photon excited fluorescence from higher electronic states of chlorophylls in photosynthetic antenna complexes: A new approach to detect strong excitonic chlorophyll *a/b* coupling. Biophys J 82: 1580–1585

Li YF, Zhou WL and Blankenship RE (1997) Crystal structure of the bacteriochlorophyll *a* protein from *Chlorobium tepidum*. J Mol Biol 271: 456–471

Limantara, L, Sakamoto S, Koyama Y and Nagae H (1997) Effects of nonpolar and polar solvents on the Q_x and Q_y energies of bacteriochlorophyll *a* and bacteriopheophytin *a*. Photochem Photobiol 65:330–337

Limantara L, Fujii R, Zhang J-P, Kanuko T, Hara H, Kawamori A, Yagura T, Cogdell RJ and Koyama Y (1998) Generation of triplet and cation-radical bacteriochlorophyll *a* in carotenoidless LH1 and LH2 antenna complexes from *Rhodobacter sphaeroides*. Biochemistry 37: 17469–17486

Linnanto JM and Korppi-Tommola JEI (2000) Excitation energy-transfer in the LH2 antenna of photosynthetic purple bacteria via excitonic B800 and B850 states. J Chin Chem Soc 47: 657–665

Linnanto J and Korppi-Tommola JEI (2002) Theoretical study of excitation transfer from modified B800 rings of the LH II antenna complex of *Rps. acidophila.* Phys Chem Chem Phys 4: 3453–3460

Linnanto J, Korppi-Tommola JEI and Helenius VM (1999) Electronic states, absorption spectrum and circular dichroism spectrum of the photosynthetic bacterial LH2 antenna of *Rhodopseudomonas acidophila* as predicted by exciton theory and semiempirical calculations. J Phys Chem B 103: 8739–8750

Liu Z, Yan H, Wang K, Kuang T, Zhang J, Gui L, An X and Chang W (2004) Crystal structure of spinach major light-harvesting complex at 2.72 Å resolution. Nature 428: 287–292

Louwe RJW, Vrieze J, Hoff AJ and Aartsma TJ (1997) Toward and integral interpretation of the optical steady-state spectra of the FMO-complex of Prosthecochloris aestuarii. 2. Exciton simulations. J Phys Chem B 101: 11280–11287

Lu XY and Pearlstein RM (1993) Simulations of *Prosthecochloris* bacteriochlorophyll *a* protein optical spectra improved by parametric computer search. Photochem Photobiol 57: 86–91

Ma Y-Z, Cogdell RJ and Gillbro T (1997) Energy transfer and exciton annihilation in the B800-850 antenna complex of the photosynthetic purple bacterium *Rhodopseudomonas acidophila* (strain 10050). A femtosecond transient absorption study, J Phys Chem B 101: 1087–1095

Matsushita M, Ketelaars M and van Oijen AM (2001) Spectroscopy of the B850 band of individual light-harvesting 2 complexes of *Rhodopseudomonas acidophila*. II. Exciton states of an elliptically deformed ring aggregate. Biophys J 80: 1604–1614

Mauring K, Novoderezhkin V, Taisova A and Fetisova Z (1999) Exciton levels structure of antenna bacteriochlorophyll *c* aggregates in green bacterium *Chloroflexus aurantiacus* as probed by 1.8–293 K fluorescence spectroscopy. FEBS Lett 456: 239–242

Mauzerall D and Greenbaum NL (1989) The absolute size of a photosynthetic unit. Biochim Biophys Acta 974: 119–140

McDermott G, Prince S, Freer A, Hawthornthwaite-Lawless A, Pariz M, Cogdell R and Isaacs N (1995) Crystal structure of an integral membrane light-harvesting complex from photosynthetic bacteria. Nature 374: 517–521

Meier T, Zhao Y, Chernyak V and Mukamel S (1997) Polarons, localization, and excitonic coherence in superradiance of biological antenna complexes. J Chem. Phys 107: 3876–3893

Mostovoy MV and Knoester J (2000) Statistics of optical spectra from single-ring aggregates and its application to LH2. J Phys Chem B 104: 12355–12364

Nagarajan, V and Parson WW (1997) Excitation energy transfer between the B850 and B875 antenna complexes of *Rhodobacter sphaeroides.* Biochemistry 36: 2300–2306

Niedermeier G, Scheer H and Feick R (1992) The functional role of protein in the organization of bacteriochlorophyll *c* in chlorosomes of *Chloroflexus aurantiacus*. Eur J Biochem 204: 685–692

Novoderezhkin VI, Palacios MA, van Amerongen H and van Grondelle R (2005) Excitation dynamics in the LHCII complex of higher plants: Modeling based on the 2.72 Å crystal structure. J Phys Chem B 109: 10493–10504

Nowak, FR (1999) Beiträge der Nichtlinearen Polarisationsspektroskopie in der Frequenzdomäne zur Aufklärung ultraschneller Prozesse in photosynthetischen bakteriellen Pigment-Protein-Komplexen. PhD Thesis, University of Potsdam

Olsen JM (1998) Chlorophyll organization and function in green photosynthetic bacteria. Photochem Photobiol 67: 61–75

Owen GM and Hoff AJ (2001) Absorbance detected magnetic resonance spectra of the FMO complex of *Prosthecochloris aestuarii* reconsidered: Exciton simulations. J Phys Chem B 105: 1458–1463

Palacios MA, de Weerd FL, Ihalainen JA, van Grondelle R and van Amerongen H (2002) Superradiance and exciton (de)localization in light-harvesting complex II from green plants? J Phys Chem B 106: 5782–5787

Palsson LO, Spangfort M, Gulbinas V and Gillbro T (1994) Ultrafast chlorophyll *b*-chlorophyll *a* excitation energy transfer in the isolated light harvesting complex, LHC II, of green plants. FEBS Lett 339: 134–138

Papiz MZ, Prince SM, Hawthornthwaite-Lawless AM, McDermott G, Freer AA, Isaacs NW and Cogdell RJ (1996) A model for the photosynthetic apparatus of purple bacteria. Trends Plant Sci 1: 198–206

Pearlstein RM (1992) Theory of the optical spectra of the bacteriochlorophyll *a* antenna protein trimer of *Prosthecochloris aestuarii*. Photosynth Res 31: 213–226

Philipson KD and Sauer K (1972) Exciton interaction in a bacteriochlorophyll-protein from *Chloropseudomonas ethylica*. Absorption and circular dichroism at 77 K. Biochemistry 11: 1880–1885

Pieper J, Rätsep M, Jankowiak R, Irrgang KD, Voigt J, Renger G and Small GJ (1999) Q_y-level structure and dynamics of solubilized light-harvesting complex II of green plants: Pressure and hole burning studies. J. Phys. Chem. A 103: 2412–2421

Prokhorenko VI, Steensgaard DB and Holzwarth AR (2000) Exciton dynamics in the chlorosomal antennae of the green

bacteria *Chloroflexus aurantiacus* and *Chlorobium tepidum*. Biophys J 79: 2105–2120

Psencík J, Polívka T, Nemec P, Dian J, Kudrna J, Malý P and Hála J (1998) Fast energy transfer and exciton dynamics in chlorosomes of the green sulfur bacterium *Chlorobium tepidum*. J Phys Chem A 102: 4392–4398

Pullerits T, Hess S, Herek J and Sundström V (1997) Temperature dependence of excitation transfer in LH2 of *Rhodobacter sphaeroides*. J Phys Chem B 101: 10560–10567

Rätsep M, Blankenship RE and Small GJ (1999) Energy transfer and spectral dynamics of the three lowest energy Q_y-states of the Fenna-Matthews-Olsen antenna complex. J Phys Chem B 103: 5736–5741

Rätsep M, Hunter CN, Olson JD and Freiberg A (2005) Band structure and local dynamics of excitons in bacterial light-harvesting complexes revealed by spectrally selective spectroscopy. Photosynth Res 86: 37–48

Remelli R, Varotto C, Sandonà D, Croce R and Bassi R (1999) Chlorophyll binding to monomeric light-harvesting complex. J Biol Chem 274: 33510–33521

Renger T and May V (2000) Simulations of frequency-domain spectra: Structure-function relationships in photosynthetic pigment-protein complexes. Phys Rev Lett 84: 5228–5231

Robert B, Cogdell RJ and van Grondelle R (2003) The light-harvesting System of Purple Bacteria. In: Green BR and parson WW (eds) Light Harvesting Antennas in Photosynthesis, pp 169–194. Kluwer Academic Publishers, Dordrecht

Rogl H and Kühlbrandt W (1999) Mutant trimers of light-harvesting complex II exhibit altered pigment content and spectroscopic features. Biochemistry 38: 16214–16222

Rogl H, Schödel R, Lokstein H, Kühlbrandt W and Schubert A (2002) Assignment of spectral substructures to pigment-binding sites in higher plant light-harvesting complex LHC II. Biochemistry 41: 2281–2287

Roszak AW, Howard TD, Southall J, Gardiner AT, Law CJ, Isaacs NW and Cogdell RJ (2003) Crystal structure of the RC-LH1 core complex from *Rhodopseudomonas palustris*, Science 302: 1969–1972

Sauer K, Smith JRL and Schultz AJ (1966) The dimerization of chlorophyll *a*, chlorophyll *b*, and bacteriochlorophyll in solution. J Am Chem Soc 88: 2681–2688

Sauer K, Cogdell RJ, Prince SM, Freer A, Isaacs NW and Scheer H (1996) Structure-based calculations of the optical spectra of the LH2 bacteriochlorophyll-protein complex from *Rhodopseudomonas acidophila*. Photochem Photobiol 64: 564–576

Savikhin S, Buck DR, Struve WS, Blankenship RE, Taisova AS, Novoderezhkin VI and Fetisova ZG (1998a) Excitation delocalization in the bacteriochlorophyll *c* antenna of the green bacteria *Chloroflexus aurantiacus* as revealed by ultrafast pump-probe spectroscopy. FEBS Lett 430: 323–326

Savikhin S, Buck DR and Struve WS (1998b) Toward level-to-level energy transfers in photosynthesis: The Fenna-Matthews-Olsen-Protein. J Phys Chem B 102: 5556–5565

Savikhin S, Buck DR and Struve WS (1999) The Fenna-Matthews-Olsen protein: A strongly coupled photosynthetic antenna. In: Andrews DL and Demidov AA (eds) Resonance energy transfer, pp 399–434. John Wiley & Sons Ltd, Chichester

Scholes GD and Fleming GR (2000) On the mechanism of light-harvesting in photosynthetic purple bacteria: B800 to B850 energy transfer. J Phys Chem B 104: 1854–1868

Scholes, GD, Gould IR, Cogdell RJ and Fleming GR (1999) *Ab initio* molecular orbital calculations of electronic couplings in the LH2 bacterial light-harvesting complex of *Rps. acidophila.* J Phys Chem B 103: 2543–2553

Schubert A, Beenken W, Stiel H, Voigt B, Leupold D and Lokstein H (2002) Excitonic coupling of chlorophylls in the plant light-harvesting complex LHC II. Biophys J 82 1030–1039

Standfuss J, Terwisscha van Scheltinga AC, Lamborghini M and Kühlbrandt W (2005) Mechanisms of photoprotection and nonphotochemical quenching in pea light harvesting complex at 2.5 Å resolution. EMBO J 24: 919–928

Stiel H, Leupold D, Teuchner K, Nowak F, Scheer H and Cogdell RJ (1997) One- and two-exciton bands in the LH2 antenna of *Rhodopseudomonas acidophila*. Chem Phys Lett 276: 62–69

Sturgis JN and Robert B (1996) The role of chromatophore coupling in tuning the spectral properties of peripheral light-harvesting protein of purple bacteria. Photosynth Res 50: 5–10

Trinkunas G, Connelly JP, Müller MG, Valkunas L and Holzwarth AR (1997) Model for the excitation dynamics in the light-harvesting complex II from higher plants. J Phys Chem B 101: 7313–7320

Tronrud DE and Matthews BW (1993) Refinement of the structure of a water-soluble antenna complex from green photosynthetic bacteria by incorporation of the chemically determined amino acid sequence. In: Deisenhofer J and Norris JR (eds) The Photosynthetic Reaction Center, Vol I, pp 13–22. Academic Press, New York

van Amerongen H and van Grondelle R (2001) Understanding the energy transfer function of LHC II, the major light-harvesting complex of green plants. J Phys Chem B 105: 604–617

van Amerongen H, Valkunas L and van Grondelle R (2000) Photosynthetic Excitons. World Scientific Publishing, Singapore

van Noort PI, Zhu Y, LoBrutto R and Blankenship RE (1997) Redox effects on the excited-states lifetime in chlorosomes and bacteriochlorophyll *c* oligomers. Biophys J 72: 316–325

van Oijen AM, Ketelaars M, Köhler J, Aartsma TJ and Schmidt J (1999) Unraveling the electronic structure of individual photosynthetic pigment-protein complexes. Science 285: 400–402

Voigt J, Renger T, Schödel R, Schrötter T, Pieper J and Redlin H (1996) Excitonic effects in the light harvesting Chl *a/b*-protein complex of higher plants. Physica status solidi B 194: 333–350

Voigt B, Irrgang K-D, Ehlert J, Beenken W, Renger G, Leupold D and Lokstein H (2002) Spectral substructure and excitonic interactions in the minor Photosystem II antenna complex CP29 as revealed by non-linear polarization spectroscopy in the frequency domain. Biochemistry 41: 3049–3056

Vulto SIE, de Baat MA, Louwe RJW, Permentier HP, Neef T, Miller M, van Amerongen H and Aartsma TJ (1998a) Exciton simulations of optical spectra of the FMO complex from the green sulfur bacterium *Chlorobium tepidum* at 6 K. J Phys Chem B 102: 9577–9582

Vulto SIE, Neerken S, Louwe RJW, de Baat MA, Amesz J and Aartsma TJ (1998b) Excited-state structure and dynamics in FMO antenna complexes from photosynthetic green sulfur bacteria. J Phys Chem B 102: 10630–10635

Walz T, Jamieson SJ and Bowers CM (1998) Projection structures of the three photosynthetic complexes from *Rhodobacter sphaeroides*: LH2 at 6 Ångstrom, LH1 and RC-LH1 at 25 Ångstrom. J Mol Biol 282: 833–845

Wendling M, Przyjalgowski MA, Gülen D, Vulto SIE, Aartsma TJ, van Grondelle R and van Amerongen H (2002) The quantita-

tive relationship between structure and polarized spectroscopy in the FMO complex of *Prosthecochloris aestuarii*: Refining experiments and simulation. Photosynth Res 71: 99–123

Westerhuis WHJ, Sturgis JN, Ratcliffe EC, Hunter CN and Niederman RA (2002) Isolation, size estimates and spectral heterogeneity of an oligomeric series of light-harvesting 1 complexes from *Rhodobacter sphaeroides*. Biochemistry 41: 8698–8707

Wolf H and Scheer H (1973) Stereochemistry and chiroptic properties of pheophorbides and related compounds. Ann NY Acad Sci 206: 549–567

Wu HM and Small GJ (1997) Symmetry adapted basis defect patterns for analysis of the effects of energy disorder on cyclic arrays of coupled chromophores. Chem Phys 218: 225–234

Wu HM and Small GJ (1998) Symmetry-based analysis of the effects of random energy disorder on the excitonic level structure of cyclic arrays: Application to photosynthetic antenna complexes. J Chem Phys B 102: 888–898

Yakovlev A, Novoderezhkin V, Taisova A and Fetisova Z (2002) Exciton dynamics in the chlorosomal antenna of the green bacterium *Chloroflexus aurantiacus*: Experimental and theoretical studies of femtosecond pump-probe spectra. Photosynth Res 71: 19–32